coatings

MDPI

Article

The Effect of Various Surface Treatments of Ti6Al4V on the Growth and Osteogenic Differentiation of Adipose Tissue-Derived Stem Cells

Jana Stepanovska [1,2,*,†], Roman Matejka [1,2,†], Martin Otahal [3], Jozef Rosina [1] and Lucie Bacakova [2]

1 Department of Biomedical Technology, Faculty of Biomedical Engineering, Czech Technical University in Prague, Sitna 3105, 272 01 Kladno, Czech Republic; roman.matejka@fbmi.cvut.cz (R.M.); rosina@fbmi.cvut.cz (J.R.)
2 Department of Biomaterials and Tissue Engineering, Institute of Physiology of the Czech Academy of Sciences, Videnska 1083, 142 20 Prague 4, Czech Republic; lucie.bacakova@fgu.cas.cz
3 Department of Natural Sciences, Faculty of Biomedical Engineering, Czech Technical University in Prague, Sitna 3105, 272 01 Kladno, Czech Republic; martin.otahal@fbmi.cvut.cz
* Correspondence: jana.stepanovska@fbmi.cvut.cz; Tel.: +420-224-35-9936
† These authors contributed equally to the study.

Received: 17 July 2020; Accepted: 3 August 2020; Published: 5 August 2020

Abstract: The physical and chemical properties of the material surface, especially its roughness and wettability, have a crucial effect on the adhesion, proliferation, and differentiation of cells. The aim of this study is to select the most appropriate surface modifications of Ti6Al4V implants for pre-colonization of the implants with adipose tissue-derived stem cells (ASCs) in order to improve their osseointegration. We compared the adhesion, growth, and osteogenic differentiation of rat ASCs on Ti6Al4V samples modified by methods commonly used for preparing clinically used titanium-based implants, namely polishing (PL), coating with diamond-like carbon (DLC), brushing (BR), anodizing (AND), and blasting (BL). The material surface roughness, measured by the Ra and Rq parameters, increased in the following order: PL < DLC < BR < AND < BL. The water drop contact angle was in the range of 60–74°, with the exception of the DLC-coated samples, where it was only 38°. The cell number, morphology, mitochondrial activity, relative fluorescence intensity of osteogenic markers RUNX2, type 1 collagen, and osteopontin, the calcium consumption by the cells and the alkaline phosphatase activity depended on the surface roughness rather than on the surface wettability of the materials. Materials with a surface roughness of several tens of nanometers (Ra 60–70 nm), i.e., the BR and AND samples, supported a satisfactory level of cell proliferation. At the same time, they achieved the highest level of osteogenic cell differentiation. These surface modifications therefore seem to be most suitable for pre-colonization of Ti6Al4V implants with stem cells pre-differentiated toward osteoblasts, and then for implanting them into the bone tissue.

Keywords: adipose-derived mesenchymal stem cells; osseointegration; osteogenic differentiation; roughness; Ti6Al4V; titanium treatments; wettability

1. Introduction

Titanium alloys, especially Ti6Al4V, are frequently used materials for bone and dental implants because of their high tensile strength, high corrosion resistance, inertness to body fluids, and biocompatibility [1]. The surface of titanium-based implants is very reactive to oxygen, which leads to the spontaneous formation of a protective film of titanium oxides (TiO_2, TiO_3, or TiO), which is constantly renewed and is thermodynamically stable. The oxide layer is well-adhesive for the calcium

and phosphate ions necessary for the mineralization of newly formed bone tissue [2]. Another important effect of the oxide layer is that it limits the leakage of metal compounds from the implant into the surrounding bone tissue. However, it does not completely prevent leakage, as there is slow passive diffusion of these compounds through the oxide layer [3]. Last but not least, titanium oxides, especially TiO_2, are known to increase the wettability of the material, to promote the adsorption of cell adhesion-mediating molecules in a physiological geometrical conformation, and to enhance the adhesion of bone cells [4].

Osteoconduction, i.e., the process of adhesion and growth of osteoblasts and progenitor cells on the implant surface, is crucial for achieving osseointegration of the implant. Osseointegration is defined as the ability of an implant to anchor directly into the surrounding bone tissue without forming an interlayer of fibrous tissue [5]. Biocompatibility is closely related to the surface characteristics of the implant, namely its roughness, wettability, chemical composition, surface topography, electrical charge, and electrical conductivity [6]. Various treatment methods have been developed to improve the surface properties of titanium-based materials for colonization with bone cells. Generally, they can be divided into physical, mechanical, chemical, biological, and combined methods. An important aim of all these methods is to roughen the surface of the implant [7]. This is believed to increase the adhesion, growth, and metabolic activity of bone cells [8], resulting in improved bone-implant attachment, increased mechanical resistance of the bone-implant contact, and long-term stability of the implant [9]. However, the optimal properties of a titanium surface, especially its roughness, have not yet been fully defined [10] (for a detailed review of currently used titanium surface treatments, see [2]).

Tissue engineering is an interdisciplinary field combining the principles of materials and cell transplantation to develop the optimal substitute for the desired tissue and/or to promote endogenous tissue regeneration [11]. In accordance with this idea, the biocompatibility and the osseointegration of titanium implants can be improved not only by various physical, chemical, and other conventionally used treatments of the implant surface, but also by recruiting stem cells on to the implant surface, and pre-differentiating them toward osteoblasts already before implantation. In this spirit, several experiments have been performed using a combined in vitro and in vivo approach. For example, in a study by Bollman et al. [12], the osseointegration of 3D-printed titanium implants with interconnected tubular structures, loaded with stromal cell-derived factor-I alpha, was markedly improved when these implants were pre-colonized with human bone marrow mesenchymal stem cells (MSCs) before they were implanted into the skull bone of rabbits [12]. Yu et al. [13] developed a complex of a titanium implant and a sheet of MSCs, where the anodized implant was enwrapped with a pre-cultivated cell sheet and was implanted into the rat tibia. In comparison with the traditional cell-free titanium implant, microCT analysis showed that the bone volume ratio and the trabecular thickness increased, while the trabecular separation decreased, in the group with the MSC-titanium complex. In accordance with these results, a histological examination revealed a greater amount of new bone tissue around the MSC-implant complexes and greater bone-implant contact [13]. An in vitro study by Sushmita et al. [14] further confirmed that it is advantageous to construct a cell-modified implant in order to achieve improved osseointegration. Specifically, dental pulp stem cell sheets were wrapped around smooth Ti implants and sandblasted large-grit acid-etched (SLA) Ti implants [14]. Both types of surfaces supported cell colonization, but the smooth surface showed greater cell growth and extracellular matrix formation than the SLA surface [14]. In another in vitro study, a comparison of the behavior of human MSCs on anodized titanium samples with nanopores of various sizes revealed that pores about 30–50 nm in diameter promoted early osteoblastic gene expression even without osteogenic supplements in the culture medium [15].

It is therefore evident that the behavior of stem cells pre-seeded on the implant surface can be controlled by appropriate surface modifications to the material. Thorough development and tests on materials with these modifications with stem cells in vitro should precede tests on animal models in vivo, in accordance with the 3R principle of ethical use of animals in testing (i.e., replacement, reduction, refinement). In addition, not only the adhesion and growth, but also the osteogenic

differentiation of stem cells should be induced by modifications to the material surface. Knowledge about the promotion of implant osseointegration by stem cells is rather sporadic, but it has been revealed that the insertion of undifferentiated dental pulp stem cells between a titanium-based implant and rat tail vertebrae delayed the osseointegration of the implant [16]. Conversely, if these cells were pre-differentiated toward osteoblasts, the osseointegration process was accelerated [16].

Based on the knowledge that we have gathered, we decided to compare the adhesion, growth, and osteogenic differentiation of rat adipose-derived mesenchymal stem cells on Ti6Al4V samples modified by methods widely used for preparing clinically used titanium-based implants, namely polishing, coating with diamond-like carbon, brushing, anodizing, and blasting. The behavior of cells in cultures on these surfaces was correlated with the surface roughness and the wettability of the material. We found that the cell behavior was governed preferentially by the surface roughness, which reached optimal values on brushed (BR) and anodized (AND) surfaces. On these surfaces, the Ra and Rq parameters, i.e., the most widely used parameters of material surface roughness, were within the range of several tens (i.e., 6–9 tens) of nanometers. On these surfaces, the cells reached the highest level of osteogenic cell differentiation and, at the same time, they maintained the good proliferation activity that is necessary for creating sufficient bone mass for proper implant osseointegration.

2. Materials and Methods

2.1. Ti6Al4V Samples and Their Modification, Characterization, and Cleaning

The substrates were custom-made of Ti6Al4V, grade 5 ELI, by Prospon s.r.o. company (Kladno, Czech Republic). Surface treatment was applied, namely polishing (PL), coating with diamond-like carbon (DLC), brushing (BR), anodizing (AND), and blasting (BL). The parameters of all surface treatments are listed in Table 1. The substrates were disc-shaped, 15 mm in diameter and 1 mm in thickness. Microscopic glass coverslips (GL) were used as a reference material.

Table 1. Titanium surface treatment parameters.

Polished	Polishing paste with granularity 3000 + felt disc
DLC	Polishing paste with granularity 3000 + felt disc + Cr-DLC layer 2–4 μm in thickness
Brushed	Brush disc, grit 320
Anodized	Polishing paste with granularity 3000 + felt disc + oxidative layer (voltage 95 V)
Blasted	F60 white corundum abrasive

The morphology of the material surface was characterized using the contact mode of atomic force microscopy (NanoWizard® 3 NanoOptics AFM System, JPK BioAFM Business, Berlin, Germany). The roughness of the substrates was analyzed by MountainsSPIP®software (version 6.7.9, Image Metrology A/S, Lyngby, Denmark); three samples for each treatment were analyzed (Figure 1). The wetting properties of the samples were evaluated using sessile drop contact angle measurements, two liquids were used, i.e., deionized water and Ringer's solution. Three samples for each treatment were analyzed and ten measurements were performed on each sample. Microscopic images were captured by a Dino-Lite system (AM4115TF, AnMo Electronics, New Taipei City, Taiwan), and the water drop contact angles were analyzed by ImageJ software, plugin Dropsnake (Figure 2), from three samples of each treatment. Microscopic glass coverslips, which are regarded as standard cultivation substrates (similarly as tissue culture polystyrene), were used as control samples for comparing the cell behavior on the tested samples. The elemental composition of the materials was analyzed by a Vanta Energy-dispersive X-ray fluorescence (ED-XRF) spectrometer (Olympus, Hamburg, Germany).

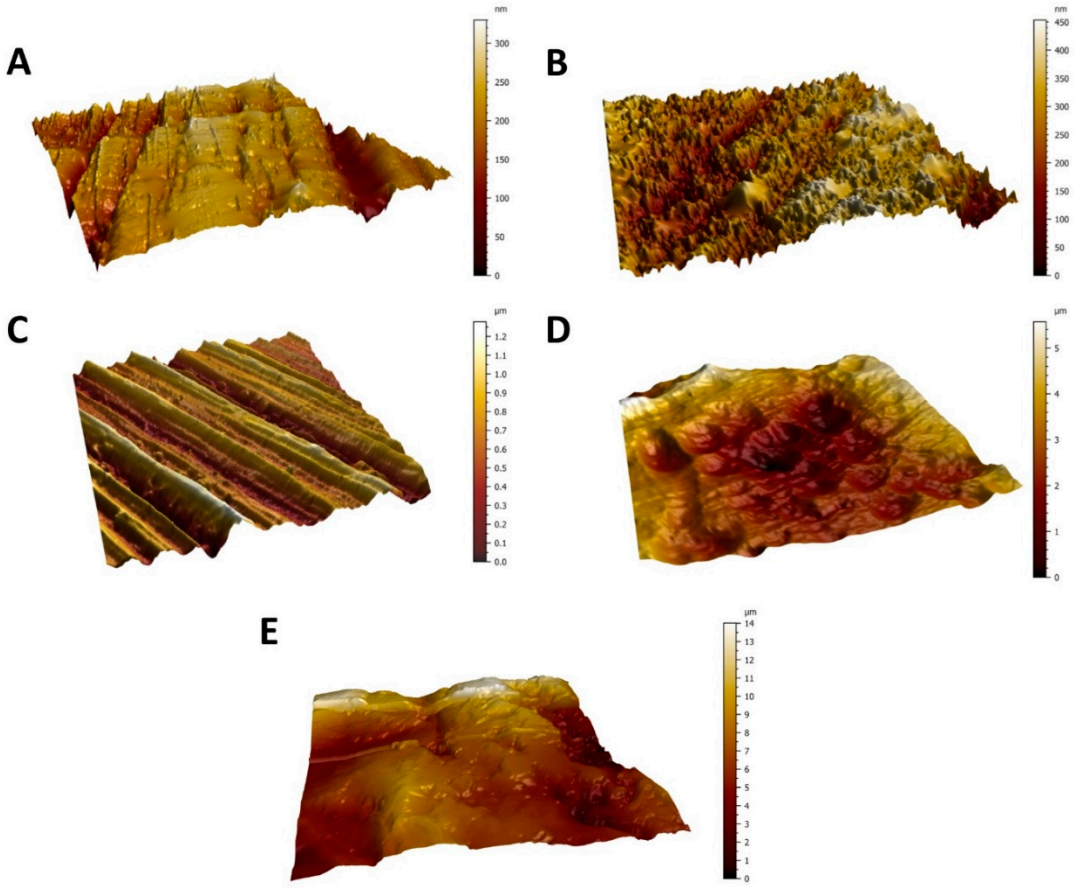

Figure 1. AFM micrographs showing the surface topography of the Ti6Al4V surfaces from the smoothest to the roughest—polished surface (**A**), diamond-like carbon (DLC)-coated surface (**B**), brushed surface (**C**), anodized surface (**D**), and blasted surface (**E**). Scanned area = 50 × 50 μm^2.

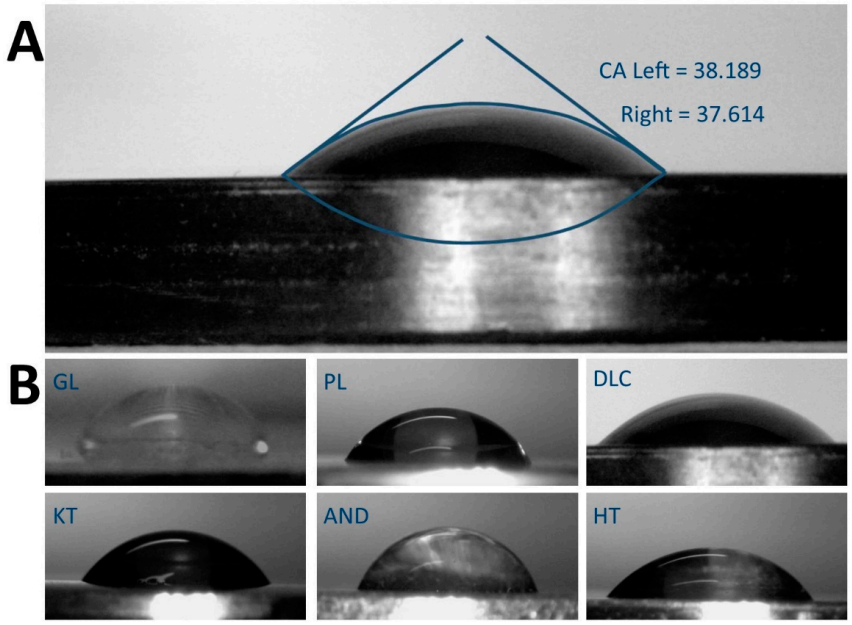

Figure 2. (**A**) Example of sessile water drop contact angle (CA) measurement on a freshly-cleaned DLC-treated surface using Dropsnake. (**B**) Water drops on all measured surfaces – reference glass coverslips (GL) and Ti6Al4V samples modified by polishing (PL), by DLC-coating (DLC), by brushing (BR), by anodizing (AND), and by blasting (BL).

In order to remove chemical residues generated during the production of the samples, and to ensure biocompatibility of the samples, all titanium substrates and glass coverslips were cleaned in 2% (*w/v*) NaOH (75 °C, 30 min), washed in ultrapure water (15 min) in a sonic bath, again cleaned in 2% (*v/v*) HNO_3 (75 °C, 30 min), and finally washed in ultrapure water in a sonic bath (15 min). Next, all substrates were dried out in an N_2 atmosphere at 60 °C for 20 min. Finally, the samples were sterilized in an autoclave (Tuttnauer, City of New York NY, USA) at 121 °C, pressure 101.3 kPa, time of the sterilization process 10 min.

2.2. Isolation and Cultivation of Rat Adipose-Derived Stem Cells

Rat adipose tissue-derived stem cells (ASCs) were used for an investigation of the adhesion, growth, and osteogenic differentiation of stem cells on the tested samples. The adipose tissue was excised from the abdominal area of male rats (Lewis, 500 g), sacrificed by an overdose of sodium thiopental anesthesia. The tissue was minced with a sterile scalpel and was digested with 0.1% collagenase type I (Gibco, Thermo Fisher Scientific, Waltham, MA, USA) for 1 h. The resulting suspension of cells was centrifuged (300 g, 5 min) five times, and after each centrifugation, the cells were washed with a sterile phosphate-buffered saline (PBS). The isolated stem cells were cultured in a growth medium consisting of a 1:1 mixture of low glucose (1 g/L) Dulbecco's modified Eagle medium and Ham's F-12 medium (DMEM/F12), both purchased from Sigma-Aldrich, St. Louis, MO, USA. The medium was supplemented with 10% of fetal bovine serum, 10 ng/mL of FGF2, and 1% of ABAM antibiotics (100 IU/mL of penicillin, 100 μg/mL of streptomycin, and 0.25 μg/mL of Gibco Amphotericin B; Sigma-Aldrich, MO, USA). The cells were seeded into 75 cm^2 culture flasks (TPP, CH); 400,000 cells in 12 mL of culture medium), and were cultivated at 37 °C in an air atmosphere with 5% CO_2 in a humidified incubator. The culture medium was changed every three days. Cell passaging was performed when the cells reached 80% confluence, using a 1mM EDTA solution and a 0.05% trypsin/0.5 mM EDTA solution in PBS.

For the experiments, the cells were seeded on to sterile Ti6Al4V samples and control glass coverslips inserted into 24-well culture plates (TPP, CH). The cells were seeded in a density of approx. 10,000 cells/cm^2; cells in the third passage were used. Differentiation of ASCs toward osteoblasts was induced using an osteogenic culture medium consisting of DMEM supplemented with 10% of fetal bovine serum, 1% ABAM, 50 μg/mL of ascorbic acid, 100 nM of dexamethasone, and 10 mM of β-glycerol phosphate.

2.3. Number, Morphology, and Osteogenic Differentiation of ASCs on Ti6Al4V Samples

Immunofluorescence staining of cells and tests of cell metabolic activity, of the calcium consumption from the culture medium and of the activity of alkaline phosphatase were carried out for an evaluation of the adhesion, proliferation, and osteogenic differentiation of ASCs.

2.3.1. Immunofluorescence Staining, Staining the Nuclei and the F-actin in Cells

Immunofluorescence staining of the cells was performed in order to visualize markers of early and intermediate osteogenic cell differentiation. The early markers included Runt-related transcription factor 2 (RUNX2), a protein responsible for inducing the differentiation of mesenchymal stem cells into immature osteoblasts, and type I collagen, an important protein of bone ECM, the expression of which is stimulated by RUNX2. Intermediate osteogenic markers were represented by osteopontin (OPN), also referred to as bone sialoprotein 1, i.e., an acidic and negatively charged ECM phosphoglycoprotein, which is deposited into non-mineralized matrix prior to calcification [17].

The immunostaining of all osteogenic markers was carried out in cells after 3, 6, and 8 days of cultivation. Cells were fixed using 4% paraformaldehyde (Sigma-Aldrich, St. Louis, MO, USA) for 20 min at room temperature (RT). The cell membranes were then permeabilized using 0.1% Triton X-100 in PBS for 15 min at RT. In order to block non-specific binding sites for antibodies, the samples were treated for 1 h at RT with PBS containing 0.1% of Tween 20 (PBST), 1% bovine serum albumin (BSA),

and 22.52 mg/mL of glycine. The cells were then exposed to primary mouse monoclonal antibodies, namely RUNX2 antibody (sc-101145, 0.4 µg/mL), COL1A1 antibody (sc-293182, 0.4 µg/mL), and OPN antibody (sc-21742, 0.8 µg/mL); all purchased from Santa Cruz Biotechnology, TX, USA. The primary antibodies were applied at RT overnight in humidified chambers. Together with the primary antibodies, tetramethylrhodamine (TRITC)-conjugated phalloidin, which stains the filamentous actin (F-actin) in the cell cytoskeleton, was also applied (Sigma-Aldrich, Cat. No. P1951, 2 µg/mL). As the secondary antibody, Alexa Fluor 488®-conjugated F(ab') fragment of goat anti-mouse IgG (H1L, Cat. No. A11017; diluted in PBS + 1% BSA, 1 µg/mL) was applied at RT for 180 min in humidified chambers. The samples that served as negative controls for staining were processed in the same way, but without the secondary antibody. Finally, the samples were mounted on thin glass coverslips using a mounting medium with DAPI, i.e., a nucleic acid stain (F6057, Sigma-Aldrich, MO, USA). The cells were then evaluated in an inverted fluorescence microscope (Leica DMi8, Wetzlar, DE), and images of randomly selected microscopic fields were taken. For each osteogenic marker, the same exposure and light excitation setting were used for all groups of tested samples.

In order to estimate the amount of differentiation markers in the cells, the intensity of the fluorescence of these markers in the cell images was analyzed using our custom-made LabVIEW software. The same threshold for each image of a given marker was set in order to remove the background from the image data. Then, the cumulative sum of all pixel intensities was evaluated, and the background intensity of the negative staining control was subtracted. The total immunofluorescence intensity values of each marker were normalized to the number of cells in the microscopic field. The intensity of the fluorescence of the cells on the reference glass samples was set to 1.

2.3.2. Evaluating the Number, the Metabolic Activity, and the Morphology of the Cells

The immunofluorescence pictures of cells with DAPI-counterstained cell nuclei were further utilized for evaluating the cell numbers. The cell number was assessed after 3, 6, and 8 days of cultivation, when the intensity of the fluorescence of DAPI in the cell images was measured and was compared with the values obtained on the control glass coverslips on day 3. Using this technique, the cell number was estimated in 15 microscopic fields on three samples for each experimental group and time interval, and then the cell population densities per cm^2 were calculated and the growth dynamics were evaluated.

In addition to the cell number, the cell metabolic activity (i.e., the activity of mitochondrial enzymes in the cells) was evaluated using a resazurin assay. After 3, 6, and 8 days of cell cultivation, the cells on the tested samples were incubated with 10% resazurin (R7017, Sigma-Aldrich, St. Louis, MO, USA), diluted in a phenol red-free medium for 2 h at 37 °C according to the manufacturer's instructions. For spectroscopic determination, the medium taken from the wells with the tested samples was pipetted into microcuvettes, and the absorbance (wavelength 570 nm) was measured by a spectrophotometer (WPA Lightwave II, Biochrom Ltd., Cambridge, UK). The experiments were performed in a series of four samples per experimental group and time interval. The absorbance values were normalized to the cell counts on the tested samples (i.e., they were calculated per cell), and the value on the glass control on day 3 was set as 100% of the metabolic activity.

The immunofluorescence images of cells with F-actin cytoskeleton counterstained with TRITC-conjugated phalloidin were further utilized for an evaluation of the spreading, the shape and the orientation of the cells after 3, 6, and 8 days of cultivation on the tested surfaces.

2.3.3. Evaluating the Calcium Concentration in the Culture Medium

On days 3, 6, and 8 of cultivation, the culture medium was taken from the wells with the tested samples and was analyzed for the concentration of calcium, using a calcium colorimetric assay (MAK022, Sigma Aldrich, St. Louis, MO, USA). The calcium concentration in the culture medium is a cell-nondestructive marker of osteogenesis, suitable for evaluating the osteogenic potential of tissue-engineered bone grafts before they are implanted [18]. It is known that the depletion of calcium

from the culture medium reflects its capture by cells, its deposition into the ECM, and the formation of mineralized bone matrix [18]. For the analysis, the cells on the samples were cultivated in a relatively large amount of culture medium (2 mL per well in 24-well plates). The culture medium was not changed, so that the cumulative change in the calcium concentration throughout the entire cell cultivation period could be measured. The calcium concentration in the medium was measured according the manufacturer's protocol. Briefly, the culture medium was diluted with deionized water (1:9) to a final volume of 50 µL. Then 90 µL of the chromogenic reagent and 60 µL of the calcium assay buffer were added, and the solution was gently mixed. After 10 min at RT in darkness, the absorbance of the solutions was measured at 575 nm. The results were expressed as the calcium consumption by the cells, i.e., an inverse value (1/c) of the calcium concentration in the culture medium was calculated. All results were standardized to the reference values obtained from the glass samples.

2.3.4. Evaluating the Activity of Alkaline Phosphatase in the Cells

The activity of alkaline phosphatase (ALP), i.e., an enzyme participating in bone matrix mineralization, was evaluated in cells on the tested samples as another important marker of osteogenic cell differentiation. For this analysis, lysates were prepared from cells after 3, 6, and 8 days of cultivation. First, the culture medium was removed from the wells, and the cells on the tested samples were washed twice with ice-cold PBS. Then an RIPA lysis buffer with a protease inhibitor in a concentration of 1:100 (HALT protease inhibitor, Thermo Fisher Scientific, Waltham, MA, USA) was applied, and the cells were scraped from the samples using a cell scraper to prepare the cell lysates. The lysates were centrifuged (15 min, 14,000× g, 4 °C) and the supernatants were stored at −20 °C. The ALP activity in the cell lysates was measured 3, 6, and 8 days after cell seeding, using an enzyme-linked immunosorbent assay (ELISA) with the alkaline phosphatase yellow (pNPP) liquid substrate system (P7998, Sigma-Aldrich, MO, USA). The reaction was stopped after 60 min from its start by an equal amount of 5M NaOH. The absorbance was measured at 405 nm by a TECAN reader (Infinite 200 PRO, Tecan, Männedorf, Switzerland).

2.4. Statistical Analysis

The results are presented as the arithmetical averages ± standard deviation (SD) from three experiments performed in duplicate or in triplicate. For each experiment, cells isolated from one animal were used. The statistical significance was evaluated using parametric one-way analysis of variance ranks and ANOVA to compare the results obtained from several groups of samples. The differences among the experimental groups were considered significant at $p \leq 0.05$.

3. Results

3.1. Surface Roughness, Wettability, and Elemental Composition of the Modified Ti6Al4V Samples

The effect of various treatments of Ti6Al4V on the surface roughness and the wettability of the material is shown in Figure 3. The roughness (Figure 3A) is described by the Ra parameter, defined as the arithmetic average of the absolute values of the profile heights along the sampling length, by the Rq parameter, which is the root mean square roughness and by RSm parameter, which defines the mean value of the width of the profile irregularities. Parameters Ra and Rq showed that the surface roughness of the modified Ti6Al4V samples increased in the following order: polished samples < DLC-coated samples < brushed samples < anodized samples < blasted samples. At the same time, the roughness of the blasted samples was in the submicron-scale, while the roughness of the other Ti6Al4V samples was in the nanoscale, which is defined by irregularities less than or equal to 100 nm in size. The reference glass coverslips were completely flat and displayed almost zero roughness (Figure 3A). The mean spacing of profile irregularities was in the micrometer scale and slightly increases with profile roughness, but these differences were not statistically significant.

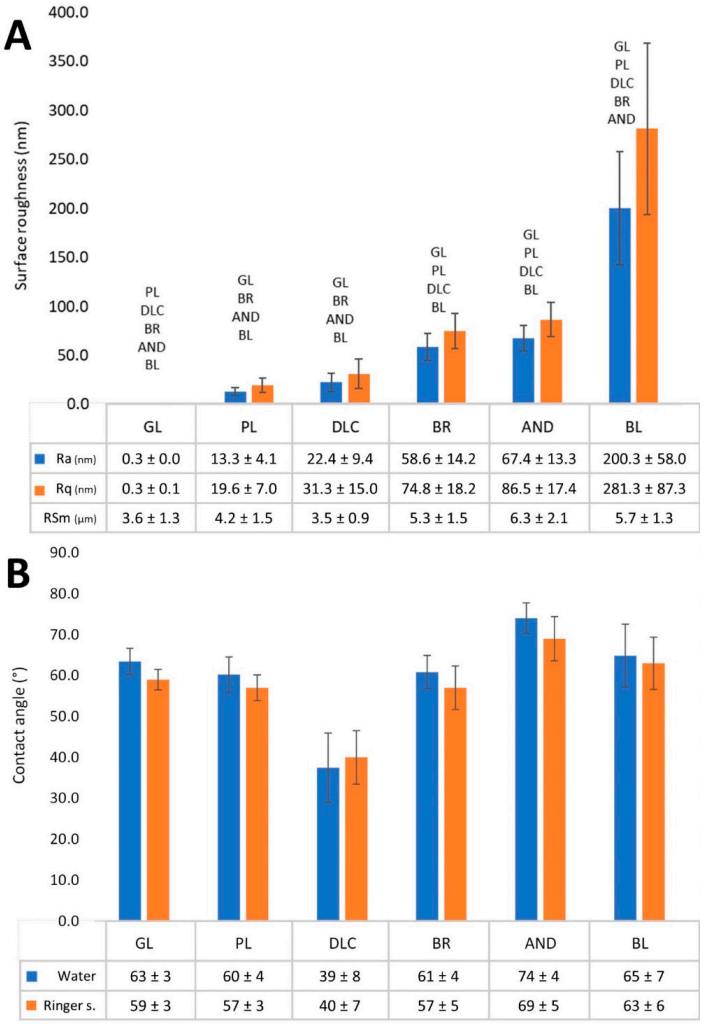

	GL	PL	DLC	BR	AND	BL
Ra (nm)	0.3 ± 0.0	13.3 ± 4.1	22.4 ± 9.4	58.6 ± 14.2	67.4 ± 13.3	200.3 ± 58.0
Rq (nm)	0.3 ± 0.1	19.6 ± 7.0	31.3 ± 15.0	74.8 ± 18.2	86.5 ± 17.4	281.3 ± 87.3
RSm (µm)	3.6 ± 1.3	4.2 ± 1.5	3.5 ± 0.9	5.3 ± 1.5	6.3 ± 2.1	5.7 ± 1.3

	GL	PL	DLC	BR	AND	BL
Water	63 ± 3	60 ± 4	39 ± 8	61 ± 4	74 ± 4	65 ± 7
Ringer s.	59 ± 3	57 ± 3	40 ± 7	57 ± 5	69 ± 5	63 ± 6

Figure 3. (**A**) Surface roughness values—average surface roughness (Ra), root mean square roughness (Rq), and mean value of the width of the profile irregularities (RSm) of the reference glass coverslips (GL) and of the Ti6Al4V samples modified by polishing (PL), by DLC-coating (DLC), by brushing (BR), by anodizing (AND), or by blasting (BL). (**B**) Wettability of the samples measured by the contact angle of a sessile drop of deionized water or Ringer's solution on a freshly cleaned surface in air. Average ± SD from three samples (10 measurements on each sample), ANOVA, statistical significance $p \leq 0.05$.

The water drop contact angle of most of the Ti6Al4V samples ranged from 60° to 75°, which indicated that these samples had similar wettability to the reference glass coverslips, which are regarded as standard cell cultivation substrates (Figure 3B). Only the wettability of the AND samples was slightly lower (contact angle greater than 74°), but this difference was not significant in comparison with the glass coverslips. However, the contact angle of the DLC-modified samples (37°) was significantly lower than on the other samples, which indicated that these samples had the greatest wettability. The measuring of the contact angle by Ringer's solution showed a higher similar trend of differences among the samples as in the water, i.e., the lowest contact angle was measured on the DLC sample, while the highest contact angle was found on the AND sample, but values of angles were slightly lower. However, this difference was not significant (Figure 3B).

Table 2 shows the elemental composition of the tested Ti6Al4V samples with various surface modifications. In DLC samples, the ED-XRF showed a relatively high presence of chromium, which was used as a base for improving the adhesion of the DLC layer doped by tungsten to the Ti6Al4V substrate. Other elements (Fe, Ni, Zn) were present only in trace amounts. These residues originally come from the production process (anodizing bath, cutting tools).

Table 2. The relative elemental composition in the surface layer of Ti6Al4V, grade 5 ELI, modified by polishing (PL), by DLC-coating (DLC), by brushing (BR), by anodizing (AND), or by blasting (BL), calculated from ED-XRF.

	Al (%)	Ti (%)	V (%)	Cr (%)	Fe (%)	Ni (%)	Zn (%)	W (%)
PL, BR, BL	5.63	89.8	4.37	0	0.20	0	0	0
AND	5.73	90.02	4.15	0	0.09	0.02	0	0
DLC	1.06	81.39	4.71	5.37	0.19	0.07	0.13	7.08

3.2. *Number and Metabolic Activity of Cells on the Modified Ti6Al4V Samples*

The effect of titanium treatment on the proliferation of ASCs is shown in Figure 4A. The cell number was estimated from the intensity of the fluorescence of the cell nuclei, which was recorded from the microscopy images of the cells on days 3, 6, and 8 of cultivation, and was normalized to the glass control on day 3. This analysis showed that, on day 3, the cell counts on the treated Ti6Al4V samples were similar to or slightly lower than on the reference glass coverslips. However, on days 6 and 8, the cell counts on all treated Ti6Al4V samples were significantly lower than on the corresponding control glass substrates ($p < 0.05$). On the polished Ti6Al4V surface, the cell population density from day 3 to 8 even remained constant, i.e., there was no increase, although on day 3 the cell counts on these samples were relatively high and were comparable with the values on glass. On the other Ti6Al4V samples, the cell number increased, but this increase was well-apparent only between days 3 and 6, while, the cell number tended to stagnate between days 6 and 8. The cell counts on the DLC, BR, and AND samples were comparable, while on the BL samples the cell counts were slightly lower (i.e., significantly lower only than on glass).

The cell metabolic activity, i.e., the activity of mitochondrial enzymes, is generally used as a marker of cell viability, and also as an indirect marker of cell number, i.e., as a value that changes in proportion to the cell number. However, in our study, this value was normalized to the cell count. Figure 4B therefore indicates the metabolic activity per cell, influenced by the properties of the cultivation substrate. This activity was lowest in the cells on the reference glass coverslips, where the cell number was relatively high. Conversely, it reached the highest values on the polished surface, where the cell counts were relatively low and were stagnating, probably because of the cells peeling off from these surfaces (Figure 5). This peeling was probably more pronounced on the samples designed for cell counting, which had undergone a more complicated staining and washing procedure than the samples designed for measuring the cell metabolic activity.

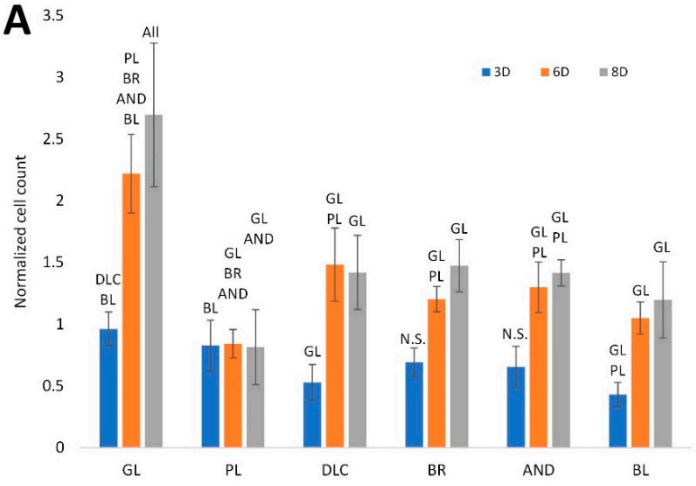

Figure 4. *Cont.*

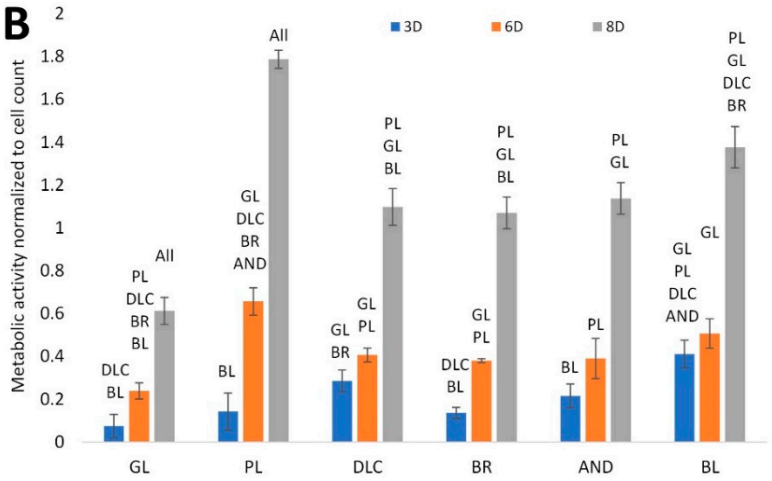

Figure 4. (**A**) Cell counts on the reference glass coverslips (GL) and on the Ti6Al4V samples modified by polishing (PL), by DLC-coating (DLC), by brushing (BR), by anodizing (AND), or by blasting (BL), estimated by the intensity of the fluorescence of the cell nuclei on microscopic images taken on days 3, 6, and 8 of cell cultivation; the values are normalized to the glass control on day 3. (**B**) Metabolic activity of cells on the control glass and on the treated titanium surfaces; the values are normalized to the cell counts. Average ± SD from 15 (cell counts)/4 (metabolic activity) samples. ANOVA, statistical significance ($p \leq 0.05$) in comparison with other experimental groups is marked by abbreviations of these groups above the columns.

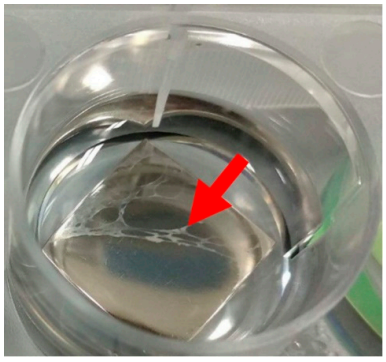

Figure 5. A cell layer peeled off the smooth surface of a polished sample (arrow). This phenomenon was observed on all samples with roughness below 25 nm, i.e., GL, PL, and DLC, but it was most noticeable on PL. These samples were excluded from the analysis.

The cell metabolic activity on the DLC, BR, and AND samples of cell nuclei on these samples reached comparable intermediate values, and the intensity of the fluorescence of the cell nuclei on these samples was also comparable. On the BL samples, however, the metabolic activity showed a tendency to reach higher values than on the DLC, BR, and AND samples, while the cell counts were relatively low. It can be therefore summarized that the metabolic activity per cell on the tested samples tended to be inversely correlated with the cell number on these samples. On all samples, there was a significant increase in the cell metabolic activity between days 6 and 8, while the main increase in the cell number was observed between days 3 and 6.

3.3. Morphology and Orientation of the Cells on Modified Ti6Al4V Samples

The cell morphology and the orientation of the cells on the tested samples was evaluated in cells stained fluorescently for F-actin in their cytoskeleton (Figure 6). The staining revealed that the cells on all investigated surfaces were well-spread with a polygonal or elongated (i.e., spindle-shaped)

morphology. The elongated morphology was apparent especially on the BR surface, where the cells, including their F-actin filaments, were oriented in parallel to the grooves in the surface of the material (Figure 6). However, some tendency toward elongation and parallel orientation of the cells was also apparent on days 6 and 8 on the control glass surfaces and on the polished Ti6Al4V surfaces, i.e., on flat surfaces with no detectable cues for cell guidance. On the DLC, AND, and BL surfaces, the cells were mostly polygonal and randomly oriented (Figure 6).

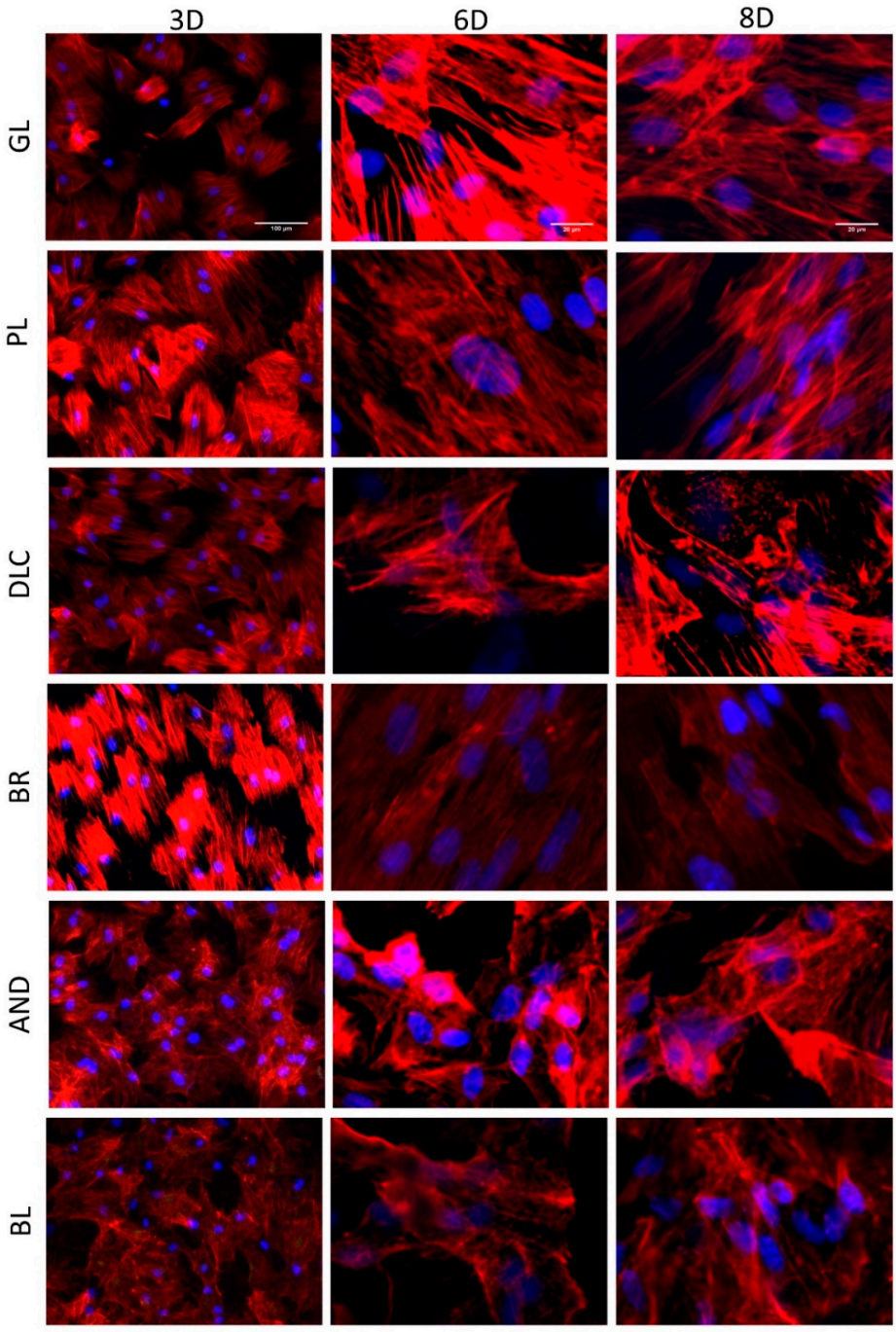

Figure 6. A comparison of the morphology of the cells on the reference glass coverslips (GL) and on the Ti6Al4V samples modified by polishing (PL), by DLC-coating (DLC), by brushing (BR), by anodizing (AND), or by blasting (BL) after 3, 6, and 8 days of cultivation. (3D, 6D, and 8D, respectively). Leica DMi8 microscope. 3D: overall picture of the cell culture, objective 10x, scale bar 100 μm; 6D, 8D: cells in detail, objective 40x, scale bar 20 μm.

3.4. Markers of Osteogenic Differentiation in Cells on the Modified Ti6Al4V Samples

The osteogenic differentiation of ASCs was investigated by immunofluorescence staining (Figure 7) of early differentiation markers RUNX2 and collagen type I (COL I), and an intermediate marker, osteopontin (OPN). The immunostaining revealed that the early markers were present in cells on all tested samples, but the amount of positively stained cells and the intensity of their staining depended on the modification of the material and on the cultivation time. The lowest fluorescence of RUNX2 and COL I was observed on the reference glass coverslips and on the polished Ti6Al4V samples on day 3 of cell cultivation, while the highest fluorescence was usually observed in cells of the BR, AND, and BL samples on day 8 (Figure 7A,B). OPN started to be visible only after 6 days of cultivation, and was clearly visible after 8 days in cells of all samples, but preferentially in the cells of the BR, AND, and BL samples (Figure 7C).

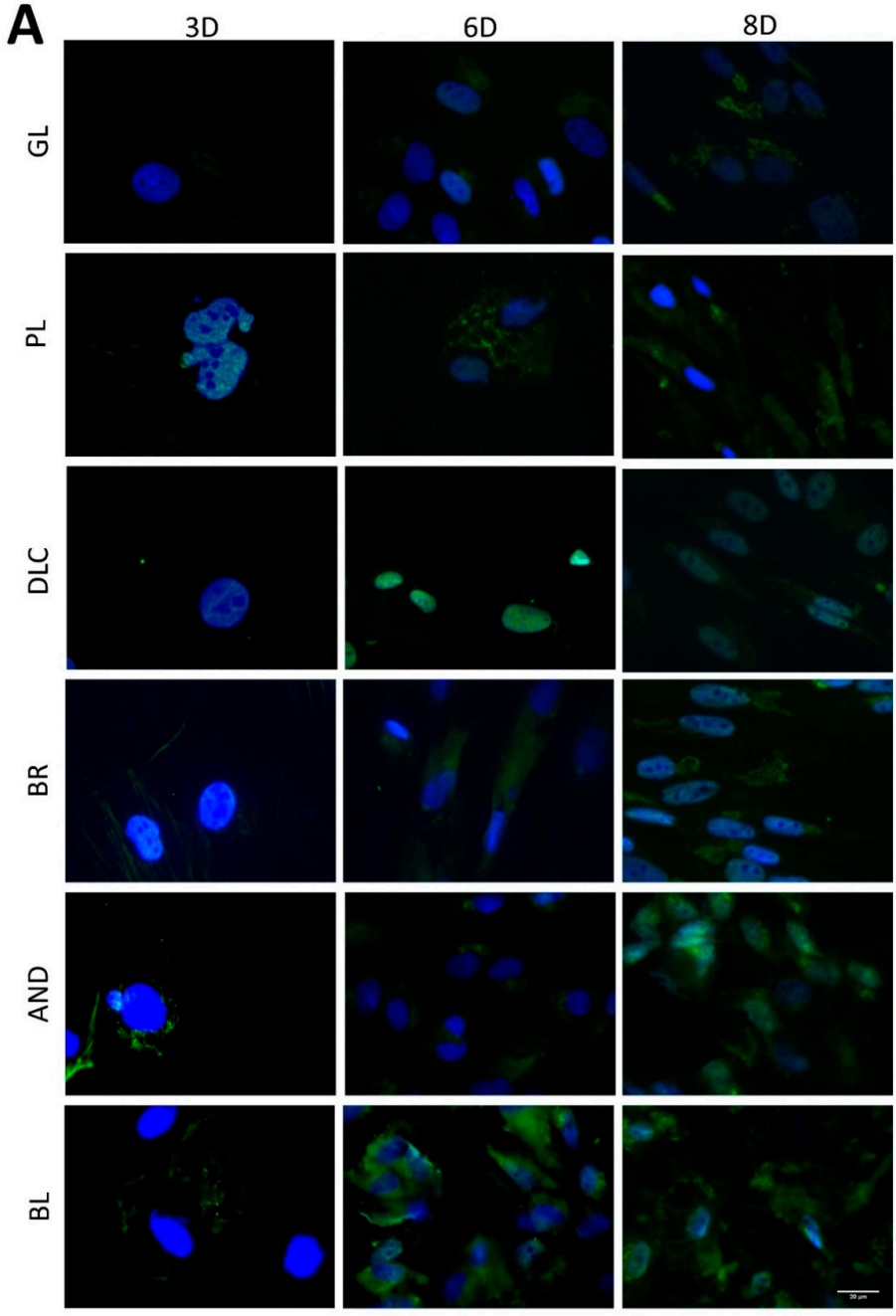

Figure 7. *Cont.*

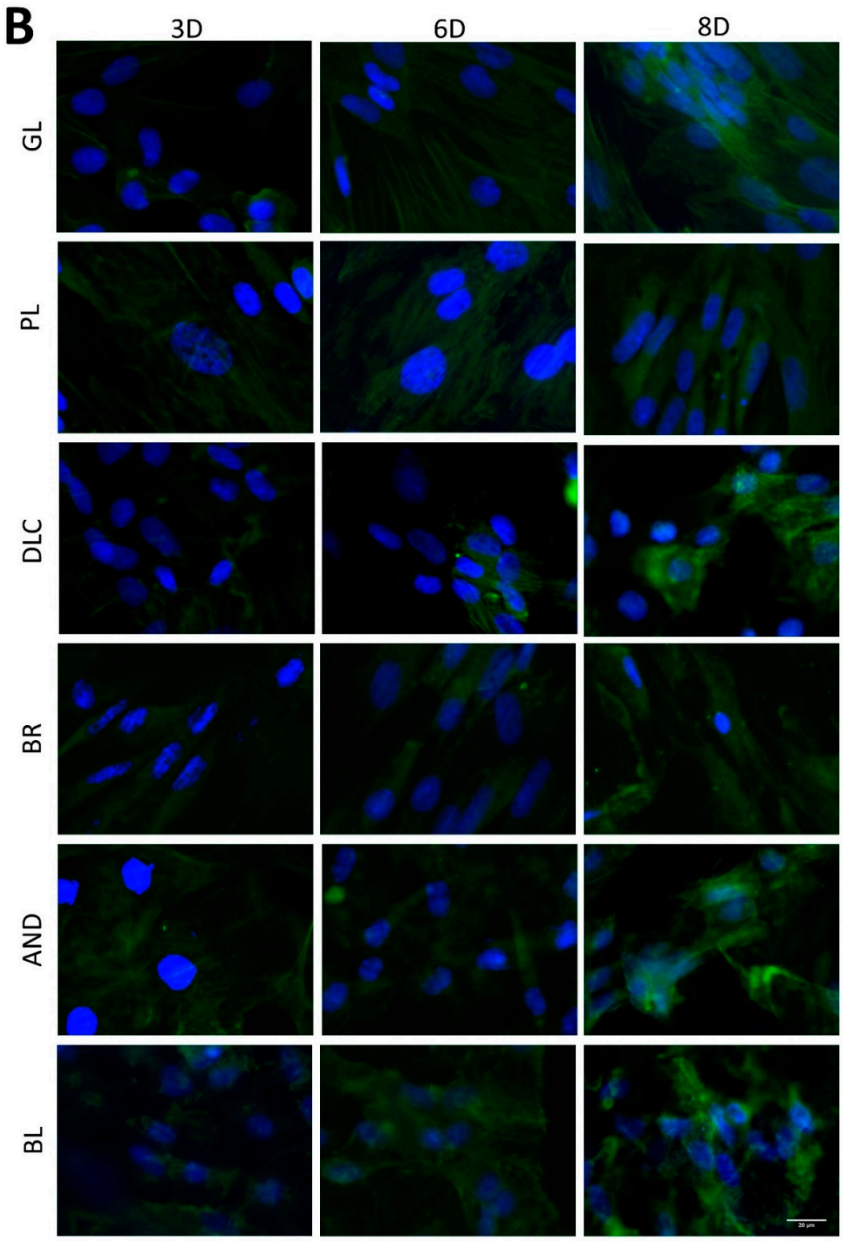

Figure 7. *Cont.*

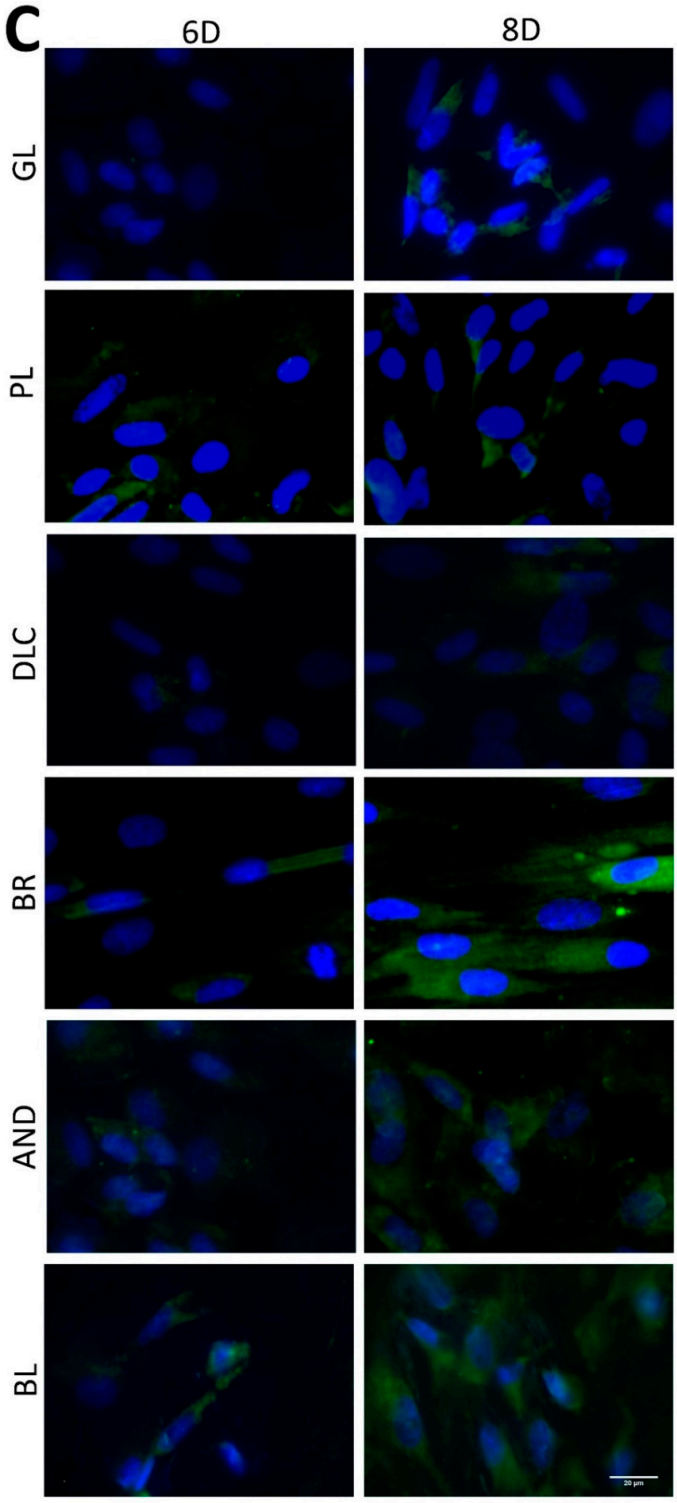

Figure 7. Immunofluorescence staining of early osteogenic markers RUNX2 (**A**) and COL1 (**B**) and an intermediate marker OPN (**C**) in cells on the reference glass coverslips (GL) and on the Ti6Al4V samples modified by polishing (PL), by DLC-coating (DLC), by brushing (BR), by anodizing (AND), or by blasting (BL) on days 3, 6, and 8 of cultivation. Leica DMi8 microscope, scale bar 20 μm.

In order to further confirm the results obtained visually from the cell images, the amount of osteogenic markers in the cells was estimated by measuring the fluorescence intensity of these markers on all samples after 3, 6, and 8 days of cultivation (Figure 8). Interestingly, the intensity of the

fluorescence of the early marker RUNX2 increased in the same order as the material surface roughness, i.e., GL < PL < DLC < BR < AND < BL (Figures 3A and 8A). The intensity of the fluorescence of COL1, another early marker of osteogenic cell differentiation, was rather similar in the cells on all tested samples, especially on day 3, but on days 6 and 8 the highest average values were obtained in cells on the AND samples (Figure 8B). Surprisingly, the values on the BL samples were relatively low, and were similar to the values on the reference glass sample. In accordance with this, the intensity of the fluorescence of OPN, an intermediate osteogenic marker, in the cells on the BL samples was also relatively low, i.e., significantly lower than on the BR samples. The intensity of the fluorescence of OPN showed a strong increasing trend similar to RUNX2, i.e., proportional to the increasing surface roughness, but it reached its maximum on the BR sample and then decreased (Figure 8C).

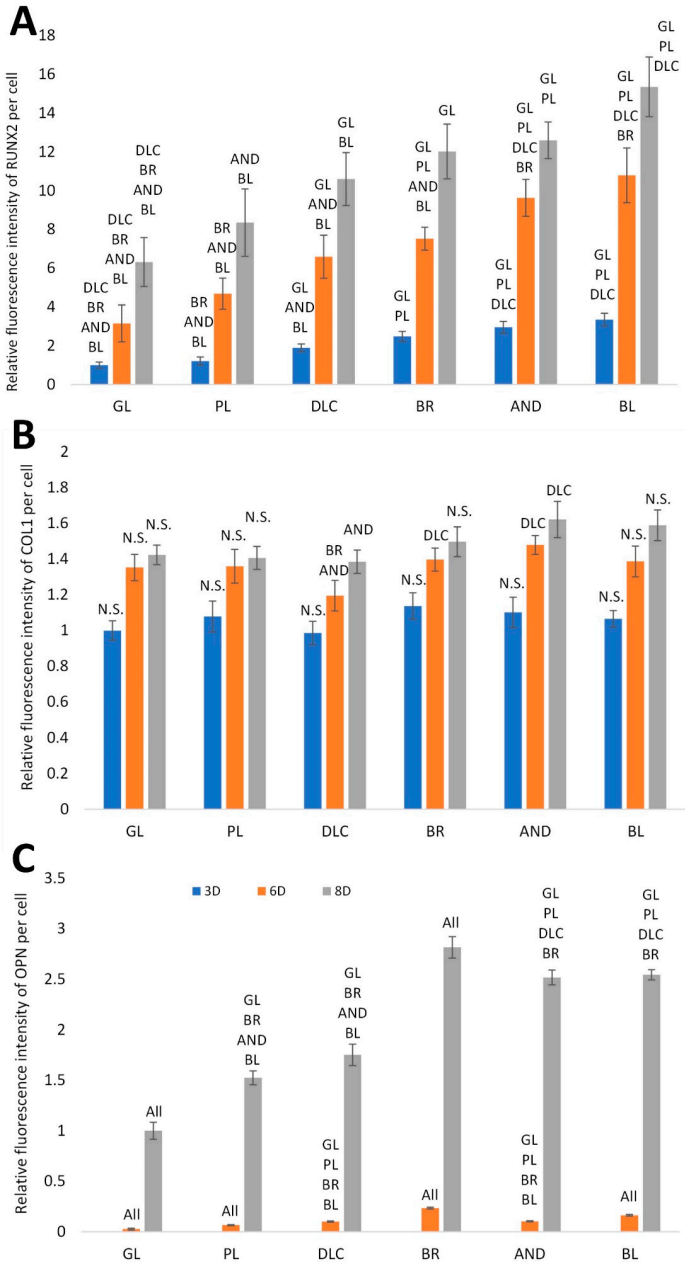

Figure 8. Relative fluorescence intensity of osteogenic markers RUNX2 (**A**), COL1 (**B**) and OPN (**C**) in cells on days 3, 6, and 8 of cultivation on the reference glass coverslips (GL) and on the Ti6Al4V samples modified by polishing (PL), by DLC-coating (DLC), by brushing (BR), by anodizing (AND), or by blasting (BL). Average ± SD from three samples, ANOVA, statistical significance ($p \leq 0.05$).

3.5. The Calcium Consumption and the Activity of Alkaline Phosphatase in Cells on the Modified Ti6Al4V Samples

Another analysis was focused on calcium consumption by cells from the culture medium, which is positively correlated with the level of cell differentiation toward osteoblasts. It can be assumed that the depletion of Ca from the culture medium is proportional to the deposition of this mineral into the ECM newly formed by the cells [18]. Our results, normalized to cell counts (Figure 9A), showed that the depletion of Ca from the culture medium increased in the same order as the surface roughness, i.e., GL < PL < DLC < BR < AND < BL, although no significant difference was found among the BR, AND, and BL samples on days 6 and 8 of cell cultivation. Only on day 3 of cell cultivation, the medium taken from the BL samples showed relatively low calcium depletion, which was comparable with the DLC and PL surfaces, but was significantly lower than on the BR and AND surfaces. The lowest calcium depletion was found in the medium from the glass control, which corresponded to the relatively low metabolic activity of the cells on this substrate. In the PL and DLC samples, the calcium depletion from the culture medium was slightly but significantly higher than for glass at later culture intervals (especially on day 6). In addition, in all tested samples, the depletion of calcium from the culture medium increased with time, i.e., from day 3 to 8, and this increase was most apparent in the BL samples (Figure 9A).

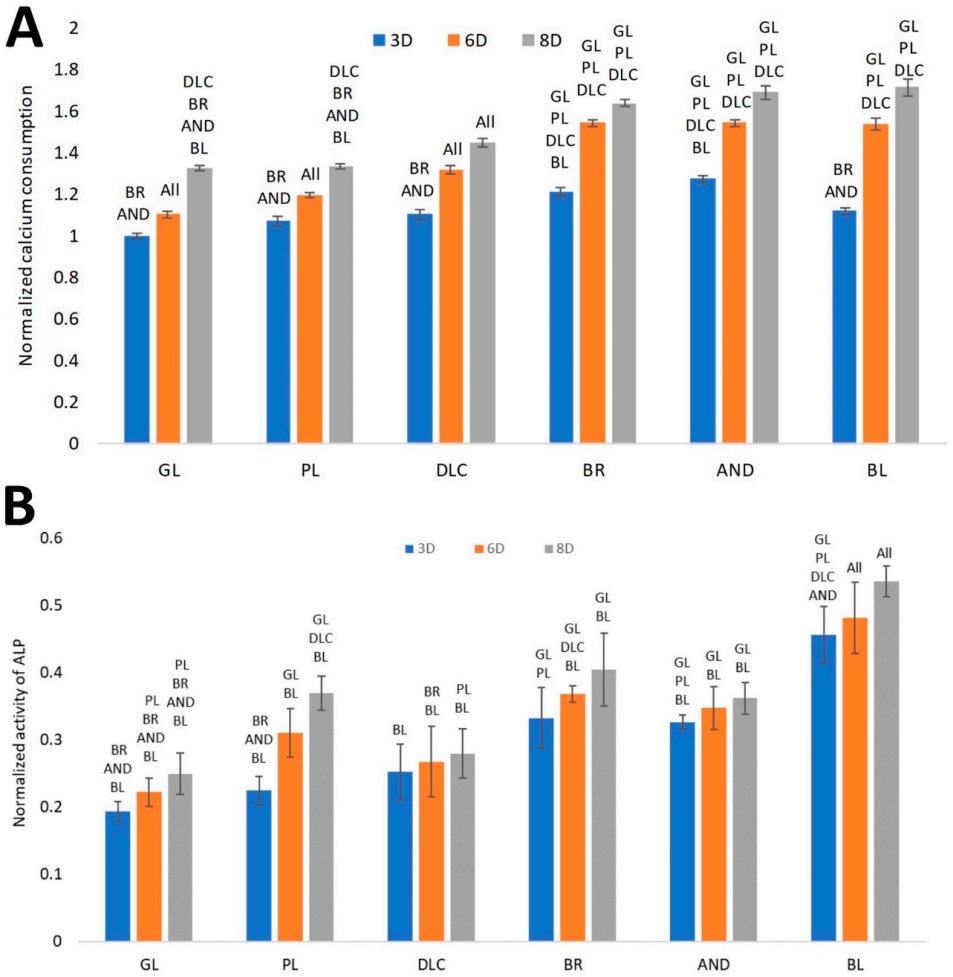

Figure 9. (**A**) Consumption of calcium from the culture medium by cells on the reference glass coverslips (GL) and on the Ti6Al4V samples modified by polishing (PL), by DLC-coating (DLC), by brushing (BR), by anodizing (AND), or by blasting (BL), estimated by the calcium depletion from the culture medium on days 3, 6, and 8 of cell cultivation. (**B**)Activity of ALP on the samples. Average ± SD from eight samples, ANOVA, statistical significance ($p \leq 0.05$).

The ALP activity, normalized to cell counts (Figure 9B), showed a similar increasing trend as for the depletion of calcium from the culture medium. The significantly highest activity of ALP was found in the cells on the BL samples, followed by the values on the BR and AND samples, which were comparable. Relatively high ALP activity (per cell) was found on the PL samples on day 8. This may have resulted from the relatively low cell count to which the activity was normalized. The lowest ALP activity was revealed in the cells on the glass samples, which corresponded with the other results obtained regarding the osteogenic cell differentiation.

3.6. A Brief Summary of the Results after 8 Days of Cultivation

The final summary of all described analyses after 8 days of cultivation is shown in Table 3. The roughness and the wettability of the material surface, the cell proliferation, the metabolic activity, and the osteogenic differentiation, represented by the production of osteogenic markers RUNX2, COL1, and OPN, the Ca consumption, and the ALP activity are compared by sorting from the highest value to the lowest value. It is apparent that higher surface roughness values (warm colors) are in general positively correlated with markers of osteogenic cell differentiation, and also with cell proliferation, which is compromised by cell detachment from the samples with lower surface roughness (cold colors). Interestingly, the roughness of the material surface and the cell performance tend to be negatively correlated with the wettability of the material, measured by the water drop contact angle.

Table 3. A summary of the results of all analyses of samples on day 8 of cell cultivation. The data are sorted according to the values of the material properties and the cell performance, from highest to lowest. All values, with the exception of roughness and wettability, are dimensionless (i.e., they are normalized to glass on day 3, with the exception of OPN, which was normalized to glass on day 8). The samples are distinguished by color according to the legend below the table.

MARKER	ROUGHNESS (nm)	CONTACT ANGLE (°)	CELL PROLIFERATION	METABOLIC ACTIVITY	OSTEOGENIC MARKERS			Ca CONSUMPTION	ALP ACTIVITY
					RUNX2	COL I	OPN		
HIGHEST LEVEL	200.3	74	2.68	1.78	15.35	1.62	2.82	1.71	0.54
	67.4	65	1.47	1.37	12.60	1.59	2.54	1.69	0.40
	58.6	63	1.42	1.13	12.02	1.49	2.51	1.63	0.37
	22.4	61	1.41	1.09	10.60	1.42	1.75	1.44	0.36
	13.3	60	1.20	1.07	8.35	1.40	1.52	1.33	0.28
LOWEST LEVEL	0.3	37	0.81	0.61	6.32	1.38	1.00	1.32	0.25

(GL PL DLC BR AND BL).

4. Discussion

In this study, we have demonstrated the influence of the surface properties of Ti6Al4V samples with various surface treatments on the adhesion, proliferation, and osteogenic differentiation of adipose-derived mesenchymal stem cells (ASCs). These treatments are currently used for clinically applied bone implants, and include polishing (PL), brushing (BR), blasting (BL), anodizing (AND), and coating with diamond-like carbon (DLC). The motivation for our study was to verify whether these commercially produced treatments are able to support desired functions in adult mesenchymal stem cells, which could be implanted together with surface-modified implants into the bone tissue of patients in order to improve the osseointegration of the implant. It has been reported that the implantation of titanium-based materials pre-seeded with mesenchymal stem cells improved the

osseointegration of these implants in rabbit [12] and rat [13] models in vivo, especially when the cells were pre-differentiated toward osteoblasts [16]. Another motivation was a common aim of tissue engineering, i.e., to test the biocompatibility and other behavior of artificial materials in biological environments according to the 3R principle, i.e., first by their interaction with cells in vitro, and then by implanting the most promising samples in vivo, and in this way to reduce the use of experimental animals. For our experiments, we used adipose tissue-derived mesenchymal stem cells (ASCs) from rats. ASCs are not typically used for osteogenic differentiation, but several studies have confirmed that these cells have considerable osteogenic and chondrogenic potential [19,20]; for a review, see [21]. On the one hand, the osteogenic potential of ASCs is lower than the osteogenic potential of bone marrow mesenchymal stem cells (bmMSCs), as revealed by our earlier study [22]. However, ASCs can be isolated in large amounts from fat tissue, which is localized subcutaneously. It is therefore relatively easily accessible by a less-invasive approach, i.e., by liposuction, whereas harvesting a large volume of bone marrow is painful and increases the risk of morbidity of the donors [23].

There have only been a limited number of studies demonstrating the adhesion, growth, and osteogenic differentiation of stem cells on titanium-based materials, and very few studies have investigated the implantation of these materials pre-colonized with stem cells pre-differentiated toward osteoblasts. Our study presented here can be regarded as pioneering work on the development of a novel modification of conventionally used metallic bone implants beyond the current state-of-the-art. The interaction between titanium-based implants and cells has been studied mainly on osteoblasts, including various lines of osteoblast-like cells often derived from bone tumors [4,8,10]; for a review, see [2,6]. The cellular response in these studies was governed by various physical and chemical surface properties of Ti-based materials, particularly by surface roughness and wettability, and also by the crystallographic orientation of the metallic materials, or by the surface charge density. According to these findings, the material surface roughness also had a pronounced effect on the behavior of ASCs in our study. Based on cell counts, flat surfaces with the Ra parameter from 0.3 to approx. 20 nm were optimal for cell adhesion and growth, which was documented by the highest cell counts achieved on glass and DLC surfaces. Interestingly, the cell counts on another flat surface, i.e., on a polished (PL) Ti6Al4V surface, showed no increasing tendency from day 3 to 8 of cultivation. This effect could be explained by the tendency of the cells to peel off from smooth surfaces, probably because of the weak adherence of cells to these surfaces (Figure 5). In addition to PL samples, this effect was also apparent on DLC surfaces and on some control glass samples, especially when well plates with the samples were handled. In this context, surface roughness of the material of several tens of nanometers (Ra approx. 60–70 nm) appeared to be more suitable for firm cell adhesion without any peeling and for subsequent cell growth, although the cell counts on the BR, AND, and BL samples were comparable to the cell counts on the DLC samples. On the BR, AND, and BL samples, the increase in the cell counts was apparent mainly between days 3 and 6, and it continued, though slowly, in the BR and AND samples up to day 8. In the DLC samples, however, the cell number showed a tendency to decrease. On the BL samples, i.e., on substrates with submicron-scale surface roughness, the cell counts were slightly lower than on the substrates with roughness in tens of nanometers. These results are in accordance with other studies, where material surface roughness in tens of nanometers is considered to be most similar to the structure of the natural bone tissue. For example, nanocrystalline diamond films with root mean square (RMS) roughness of 20 nm were more suitable for the adhesion and osteogenic differentiation of human osteoblast-like Saos-2 cells than films with RMS roughness of 270 or 500 nm, or flat polystyrene surfaces. This was explained by the greatest similarity of films with RMS 20 nm to the real bone surface [24].

The beneficial effect of nanostructured surfaces on the adhesion and growth of osteoblasts has been further attributed to the preferential adsorption of vitronectin on these surfaces, due to its relatively small and linear molecule. Vitronectin is then preferentially recognized by osteoblasts rather than by other cell types, because osteoblasts bind specifically the Lys-Arg-Ser-Arg (KRSR) sequence in the vitronectin molecule [25]. Micro-scale surface roughness (irregularities > 1 μm), originating from

mechanical machining and blasting the material surface with relatively large particles, can hamper cell adhesion, spreading and proliferation. This is due to the inappropriate size, shape, and spacing of the irregularities on the material surface relative to the cells [25].

Another important factor influencing the cell-material interaction is the wettability of the material surface. This factor is closely related to the surface roughness of the material, although there are several other factors that can influence the hydrophilicity of the surface of a material, e.g., the chemical composition of the surface. In accordance with this, the water drop contact angle of the Ti-based surfaces in our study was in the range of approx. 60° to 75°, but in case of DLC, the angle was only 38°. In numerous studies, the hydrophilicity (i.e., a lower water drop contact angle) of a material has been described as a factor increasing the adhesion and proliferation of cells. This positive effect has been explained by the adsorption of cell adhesion-mediating proteins, e.g., vitronectin and fibronectin, from the serum supplement of the culture medium in a physiological, flexible geometrical conformation, which can be well-recognized by the cell adhesion receptors and can be remodeled by the cells. Conversely, on hydrophobic surfaces, the cell adhesion-mediating proteins are adsorbed in a rigid, denatured form, which limits the binding of cell adhesion receptors [26,27]. However, our results showed that a decreased water drop contact angle, i.e., increased wettability of the DLC samples, had a rather negative effect on the adhesion, the proliferation, and especially the osteogenic differentiation of ASCs in cultures on these samples. Similar results have also been obtained in other studies focused on cell attachment to biomaterials with various levels of wettability. For example, in a study performed on plasma-treated hexamethyldisiloxane, samples with the water drop contact angle ranging from 0° to 100°, the attachment of mouse MC3T3-E1 pre-osteoblasts was highest on samples with contact angles from 60° to 80° [28], i.e., on slightly hydrophilic or even hydrophobic substrates. According to a study by Vogler et al. [29], surfaces with a water drop contact angle lower than 65°, defined as hydrophilic, exhibited short-range repulsive forces between opposing surfaces immersed in water, while surfaces with the contact angle greater than 65°, defined as hydrophobic, exhibited long-range attractive forces between the opposing surfaces [29]. Accordingly, hydrophilic surfaces were less efficient in adsorbing proteins contained in the fetal bovine serum, which is commonly used as a supplement for the standard culture media [29]. It is known that the strength and the stability of the adsorption of cell adhesion-mediating proteins from the serum in the culture medium decrease with increasing wettability of a material (for a review, see [22]). The cell adhesion is therefore optimal on moderately wettable materials, while highly hydrophilic surfaces can behave as repulsive for cells. In accordance with this, the cells on DLC samples with the lowest contact angle of 38° were prone to peel off from the surface of the material. However, cell peeling was also apparent on the PL samples and on the control glass samples, i.e., on samples with contact angles of approx. 60–65°, i.e., close to the optimal values. The peeling could therefore be attributed to low surface roughness rather than to high surface wettability. Similarly, in a study by Pivodova et al. [8], various physical treatments of titanium samples that affected the surface roughness of the material played a more important role than chemical modifications affecting the material surface wettability in the behavior of human osteoblast-like Saos-2 cells in cultures on these samples [8].

When the influence of the roughness and the wettability of the surface of the material on cell metabolic activity was assessed, the results differed markedly from the cell counts. This was because the cell metabolic activity was calculated per cell in our study. Despite high cell counts, the metabolic activity of an individual cell on the control glass coverslips was very low in comparison with the other samples. Conversely, the highest metabolic activity was observed in cells on polished samples, where the cell counts were relatively low and were stagnating. However, this result is probably distorted by the relatively low cell count measured on the PL surface, which was caused by the cells peeling off when the sample was handled. There may be more peeling during the relatively complicated immunofluorescence staining procedure, which includes more steps and more extensive washing than the measurement of cell metabolic activity. The highest metabolic activity per cell found on the PL samples therefore seems to be a false and unreal result. Another reason for the relatively low

cell counts on DLC-coated samples could be the presence of chromium in these samples, which was used for improving the adhesion of tungsten-doped DLC layer to the Ti-based substrate, and which are potentially cytotoxic. However, an earlier study performed on Cr-doped DLC films revealed that the presence of chromium did not have a considerable negative effect on the adhesion, proliferation, and viability of human osteoblast-like Saos-2 cells in cultures on these films [30]. Similarly, the DLC films enhanced with tungsten showed no considerable cytotoxicity in vitro [31].

On the DLC, BR, AND, and BL samples, both parameters, i.e., the cell counts and the cell metabolic activity, reached a similar intermediate level. However, from day 6 to 8, when the cell counts on these samples were stagnating, the metabolic activity per cell increased markedly. In this case, however, this activity probably correlated with the level of osteogenic cell differentiation. This is suggested particularly by the intensity of the fluorescence of osteopontin, an intermediate marker of osteogenic cell differentiation, which also increased markedly between days 6 and 8, reaching the highest values on the BR samples. Other markers of differentiation, such as RUNX2, calcium deposition (measured by the calcium depletion from the culture medium), and the activity of alkaline phosphatase increased more homogeneously from day 3 to 8. However, these markers were clearly positively correlated with the surface roughness of the material. The highest values of the markers were usually obtained in cells on BR, AND, and BL samples, i.e., samples with the highest surface roughness, while the values were lower in cells on the flatter PL and DLC samples, and particularly on the control glass coverslips. This is in line with the results obtained by other authors, who have reported that relatively high material surface roughness, particularly submicron- and micron-scale roughness, is associated with a high level of cell osteogenic differentiation, but with reduced cell proliferation [32–34]. The decrease in cell proliferation is sometimes so great that it cannot ensure the formation of enough bone mass around the implants for the needs of osseointegration [32]. Because of the irregularities on the material surface, the cells lose their mutual contacts, which are necessary for cell proliferation [32]. However, it seems that this did not occur in our study, because the cells remained in contact even on the roughest surfaces, and were able to reach confluence, as is evident from the cell morphology images (Figure 6). It should be mentioned here that the cell proliferation was evaluated in a medium supporting cell differentiation, where the cell proliferation activity is generally lower than in a standard growth medium.

In summary, all surface treatments applied to the Ti6Al4V samples were non-cytotoxic, supporting the adhesion, growth, and osteogenic differentiation of ASCs. Cell proliferation was most efficiently supported by relatively flat surfaces with roughness described by an Ra parameter from tenths of a nanometer to 1–2 tens of nanometers, i.e., by the glass, PL and DLC surfaces. However, this supportive effect was compromised by peeling of the cells from the samples during handling, probably because of weak cell adhesion to these smooth surfaces; the final cell counts were therefore often low. The final cell counts were also relatively low on BL surfaces with roughness (Ra) in hundreds of nanometers, i.e., on surfaces with submicron scale roughness. Satisfactory cell counts were achieved on surfaces with roughness (Ra) in 6–7 tens of nanometers, i.e., on the BR and AND surfaces. At the same time, the cells on these surfaces achieved a relatively high level of osteogenic differentiation, manifested particularly by the highest production of osteopontin. Ti6Al4V implants modified by brushing and anodizing therefore seem to be the most suitable of the samples tested here for colonizing with pre-differentiated ASCs before they are implanted into the bone tissue.

Some limitations of our study should be pointed out. The experiments were carried out only for 8 days. This is sufficient for investigating only the early stage of osteogenic cell differentiation, but not the late stage, which is characterized by osteocalcin production [33]. For late osteogenic differentiation, the cells should be cultivated for a much longer period of time, usually for three or more weeks. This type of long-term cultivation is hardly possible in a conventional static two-dimensional culture system, where the cells, especially stem cells, proliferate rapidly, and reach confluence relatively soon. They then enter the stationary phase, associated with apoptosis and cell detachment. The cell performance can be improved by using a more physiological cultivation system, including three-dimensional scaffolds, which better simulate the architecture of the tissues in vivo, and by using

dynamic cultivation, which applies mechanical loading to cells similarly as in vivo. Together with biochemical signals from the culture medium, this loading directs the cell differentiation toward a desired phenotype.

5. Conclusions

This study has investigated the influence of surface properties of Ti6Al4V with various commercially used surface modifications on the growth and the osteogenic differentiation of adipose tissue-derived mesenchymal stem cells (ASCs). The aim was to select the most appropriate surface modification(s) for pre-colonizing Ti6Al4V implants with stem cells in order to improve their osseointegration. The Ti6Al4V samples were treated by polishing (PL), by brushing (BR), by anodizing (AND), by blasting (BL), or by diamond-like carbon (DLC) coating. A glass coverslip (GL) was used as a reference material. The basic surface properties of the materials, i.e., their roughness and their wettability, were evaluated and were correlated with the behavior of ASCs cultivated on the materials for 3, 6, and 8 days in a culture medium promoting osteogenic differentiation. On materials with low surface roughness (Ra from tenths of a nanometer to 1–2 tens of nanometers), i.e., on GL, PL, and DLC, the cells adhered and proliferated very well. However, because of the smoothness of these surfaces, the cells were prone to peel off. Materials with greater surface roughness (Ra 60–70 nm), i.e., the BR and AND samples, still supported a good level of cell proliferation and, at the same time, they achieved a markedly higher level of osteogenic cell differentiation than the previous group. On surfaces with submicron-scale roughness, i.e., on the BL samples, the level of osteogenic differentiation was also relatively high, but these samples showed the lowest cell proliferation activity. All tested samples showed moderate wettability, characterized by a water drop contact angle in the optimum range of 60–80°. The only exception was the DLC samples, which were more hydrophilic (contact angle 38°). However, the differences in surface wettability did not have any significant effect on the cell behavior, which seemed to be primarily governed by the surface roughness of the material. It can therefore be concluded that TiAl4V samples treated with brushing and anodizing are the most appropriate for pre-colonizing with stem cells pre-differentiated toward osteoblast before they are implanted into the bone tissue. However, samples treated by polishing, by blasting, or by coating with DLC have some limitations that reduce their potential for use as an implant material in general.

Author Contributions: Conceptualization, J.S. and L.B.; methodology, J.S., R.M.; software, J.S., R.M.; validation, R.M., J.S. and L.B.; formal analysis, R.M., J.S.; investigation, J.S, R.M. and M.O.; resources, J.S., R.M. and L.B.; data curation, R.M. and J.S.; writing—original draft preparation, J.S. and R.M.; writing—review and editing, L.B. and J.R.; visualization, J.S. and R.M.; supervision, J.R. and L.B.; project administration, L.B.; funding acquisition, L.B. All authors have read and agreed to the published version of the manuscript.

Funding: This research was funded by the Grant Agency of the Czech Republic (project No. 20-01570S), by the Grant Agency of the Czech Technical University in Prague (No. SGS19/088/OHK4/1T/17); by the Biotechnology and Biomedicine Centre of the Academy of Sciences and Charles University (BIOCEV, project No. CZ.1.05/1.1.00/02.0109), supported by the European Regional Development Fund, and by the ENOCH Project (No. CZ.02.1.01/0.0/0.0/16_019/0000868), supported by the European Regional Development Fund.

Acknowledgments: Prospon s.r.o. company (Kladno, CZ) is gratefully acknowledged for providing Ti6Al4V samples for studies on cell-material interaction. We also thank Robin Healey (Czech Technical University in Prague, CZ) for the language revision of this manuscript.

Conflicts of Interest: The authors declare no conflict of interest.

Ethical Statement: The animal experiments carried out within this study were approved by the Ministry of Health of the Czech Republic, reference no MZDR 52084/2018-4/OVZ, approval no 87/2018. A minimal number of animals were used. All procedures described here were carried out according to ethical guidelines in order to minimize the pain and discomfort of the animals. The Institute of Clinical and Experimental Medicine has authorized facilities and fully equipped operating theaters for performing these animal experiments.

References

1. Williams, D.F. On the mechanisms of biocompatibility. *Biomaterials* **2008**, *29*, 2941–2953. [CrossRef] [PubMed]
2. Stepanovska, J.; Matejka, R.; Rosina, J.; Bacakova, L.; Kolarova, H. Treatments for enhancing the biocompatibility of titanium implants. A review. *Biomed. Pap.* **2020**, *164*, 23–33. [CrossRef] [PubMed]
3. Liu, X.; Chu, P.; Ding, C. Surface modification of titanium, titanium alloys, and related materials for biomedical applications. *Mater. Sci. Eng. R Rep.* **2004**, *47*, 49–121. [CrossRef]
4. Vandrovcova, M.; Hanus, J.; Drabik, M.; Kylian, O.; Biederman, H.; Lisa, V.; Bacakova, L. Effect of different surface nanoroughness of titanium dioxide films on the growth of human osteoblast-like MG63 cells. *J. Biomed. Mater. Res. A* **2012**, *100*, 1016–1032. [CrossRef] [PubMed]
5. Zafar, M.S.; Fareed, M.; Riaz, S.; Latif, M.; Habib, S.; Sultan, Z. Customized Therapeutic Surface Coatings for Dental Implants. *Coatings* **2020**, *10*, 568. [CrossRef]
6. Bagno, A.; Di Bello, C. Surface treatments and roughness properties of Ti-based biomaterials. *J. Mater. Sci. Mater. Med.* **2004**, *15*, 935–949. [CrossRef]
7. Liu, W.; Liu, S.; Wang, L. Surface Modification of Biomedical Titanium Alloy: Micromorphology, Microstructure Evolution and Biomedical Applications. *Coatings* **2019**, *9*, 249. [CrossRef]
8. Pivodova, V.; Frankova, J.; Dolezel, P.; Ulrichova, J. The response of osteoblast-like SaOS-2 cells to modified titanium surfaces. *Int. J. Oral Max. Impl.* **2013**, *28*, 1386–1394. [CrossRef]
9. Sakka, S.; Coulthard, P. Implant failure: Etiology and complications. *Med. Oral Patol. Oral Cir. Bucal.* **2011**, *16*, e42–e44. [CrossRef]
10. Rad, A.T.; Faghihi, S. On the Relation Between Surface Texture of Metallic Implants and Their Bioactivity. *Surf. Innov.* **2019**, *7*, 1–31. [CrossRef]
11. Furth, M.E.; Atala, A. Chapter 6-Tissue Engineering: Future Perspectives. In *Principles of Tissue Engineering*, 4th ed.; Lanza, R., Langer, R., Vacanti, J., Eds.; Academic Press: Boston, MA, USA, 2014; pp. 83–123. [CrossRef]
12. Bollman, M.; Malbrue, R.; Li, C.; Yao, H.; Guo, S.; Yao, S. Improvement of osseointegration by recruiting stem cells to titanium implants fabricated with 3D printing. *Ann. N. Y. Acad. Sci.* **2019**. [CrossRef]
13. Yu, M.; Zhou, W.; Song, Y.; Yu, F.; Li, D.; Na, S.; Zou, G.; Zhai, M.; Xie, C. Development of mesenchymal stem cell-implant complexes by cultured cells sheet enhances osseointegration in type 2 diabetic rat model. *Bone* **2011**, *49*, 387–394. [CrossRef]
14. Sushmita, V.; Chethan Kumar, J.; Hegde, C.; Kurkalli, B. Interaction of dental pulp stem cells in bone regeneration on titanium implant. An in vitro study. *J. Osseointegration* **2019**, *11*, 553–560. [CrossRef]
15. Lavenus, S.; Trichet, V.; Le Chevalier, S.; Hoornaert, A.; Louarn, G.; Layrolle, P. Cell differentiation and osseointegration influenced by nanoscale anodized titanium surfaces. *Nanomedicine* **2012**, *7*, 967–980. [CrossRef] [PubMed]
16. Perczel-Kovach, K.E.; Farkasdi, S.; Kallo, K.; Hegedus, O.; Keremi, B.; Cuisinier, F.; Blazsek, J.; Varga, G. Effect of stem cells of dental pulp origin on osseointegration of titanium implant in a novel rat vertebra model. *Fogorv. Szle.* **2017**, *110*, 7–14.
17. Tataria, M.; Quarto, N.; Longaker, M.T.; Sylvester, K.G. Absence of the p53 tumor suppressor gene promotes osteogenesis in mesenchymal stem cells. *J. Pediatr. Surg.* **2006**, *41*, 624–632. [CrossRef] [PubMed]
18. Tanikake, Y.; Akahane, M.; Furukawa, A.; Tohma, Y.; Inagaki, Y.; Kira, T.; Tanaka, Y. Calcium Concentration in Culture Medium as a Nondestructive and Rapid Marker of Osteogenesis. *Cell Transplant.* **2017**, *26*, 1067–1076. [CrossRef]
19. Im, G., II; Shin, Y.-W.; Lee, K.-B. Do adipose tissue-derived mesenchymal stem cells have the same osteogenic and chondrogenic potential as bone marrow-derived cells? *Osteoarthr. Cartilage* **2005**, *13*, 845–853. [CrossRef]
20. Grottkau, B.E.; Lin, Y. Osteogenesis of Adipose-Derived Stem Cells. *Bone Res.* **2013**, *1*, 133–145. [CrossRef]
21. Bacakova, L.; Zarubova, J.; Travnickova, M.; Musilkova, J.; Pajorova, J.; Slepicka, P.; Kasalkova, N.S.; Svorcik, V.; Kolska, Z.; Motarjemi, H.; et al. Stem cells: Their source, potency and use in regenerative therapies with focus on adipose-derived stem cells—A review. *Biotechnol. Adv.* **2018**, *36*, 1111–1126. [CrossRef]
22. Przekora, A.; Vandrovcova, M.; Travnickova, M.; Pajorova, J.; Molitor, M.; Ginalska, G.; Bacakova, L. Evaluation of the potential of chitosan/β-1,3-glucan/hydroxyapatite material as a scaffold for living bone graft production in vitro by comparison of ADSC and BMDSC behaviour on its surface. *Biomed. Mater.* **2017**, *12*, 015030. [CrossRef] [PubMed]

23. Auquier, P.; Macquart-Moulin, G.; Moatti, J.P.; Blache, J.L.; Novakovitch, G.; Blaise, D.; Faucher, C.; Viens, P.; Maraninchi, D. Comparison of anxiety, pain and discomfort in two procedures of hematopoietic stem cell collection: Leukacytapheresis and bone marrow harvest. *Bone Marrow Transplant.* **1995**, *16*, 541–547. [PubMed]
24. Kalbacova, M.; Rezek, B.; Baresova, V.; Wolf-Brandstetter, C.; Kromka, A. Nanoscale topography of nanocrystalline diamonds promotes differentiation of osteoblasts. *Acta Biomater.* **2009**, *5*, 3076–3085. [CrossRef] [PubMed]
25. Bacakova, L.; Filova, E.; Parizek, M.; Ruml, T.; Svorcik, V. Modulation of cell adhesion, proliferation and differentiation on materials designed for body implants. *Biotechnol. Adv.* **2011**, *29*, 739–767. [CrossRef] [PubMed]
26. Goddard, J.M.; Hotchkiss, J.H. Polymer surface modification for the attachment of bioactive compounds. *Prog. Polym. Sci.* **2007**, *32*, 698–725. [CrossRef]
27. Xu, L.-C.; Siedlecki, C.A. Effects of surface wettability and contact time on protein adhesion to biomaterial surfaces. *Biomaterials* **2007**, *28*, 3273–3283. [CrossRef] [PubMed]
28. Wei, J.; Igarashi, T.; Okumori, N.; Igarashi, T.; Maetani, T.; Liu, B.; Yoshinari, M. Influence of surface wettability on competitive protein adsorption and initial attachment of osteoblasts. *Biomed. Mater.* **2009**, *4*, 045002. [CrossRef]
29. Vogler, E.A. Water and the acute biological response to surfaces. *J. Biomater. Sci. Polym. Ed.* **1999**, *10*, 1015–1045. [CrossRef]
30. Jelinek, M.; Zemek, J.; Vandrovcová, M.; Bačáková, L.; Kocourek, T.; Remsa, J.; Písařík, P. Bonding and bio-properties of hybrid laser/magnetron Cr-enriched DLC layers. *Mater. Sci. Eng. C* **2016**, *58*, 1217–1224. [CrossRef]
31. Mansano, R.D.; Ruas, R.; Mousinho, A.P.; Zambom, L.S.; Pinto, T.J.A.; Amoedo, L.H.; Massi, M. Use of diamond-like carbon with tungsten (W-DLC) films as biocompatible material. *Surf. Coat. Technol.* **2008**, *202*, 2813–2816. [CrossRef]
32. Zhao, L.; Mei, S.; Chu, P.K.; Zhang, Y.; Wu, Z. The influence of hierarchical hybrid micro/nano-textured titanium surface with titania nanotubes on osteoblast functions. *Biomaterials* **2010**, *31*, 5072–5082. [CrossRef] [PubMed]
33. Gittens, R.A.; McLachlan, T.; Olivares-Navarrete, R.; Cai, Y.; Berner, S.; Tannenbaum, R.; Schwartz, Z.; Sandhage, K.H.; Boyan, B.D. The effects of combined micron-/submicron-scale surface roughness and nanoscale features on cell proliferation and differentiation. *Biomaterials* **2011**, *32*, 3395–3403. [CrossRef] [PubMed]
34. Moon, B.S.; Kim, S.; Kim, H.E.; Jang, T.S. Hierarchical micro-nano structured Ti6Al4V surface topography via two-step etching process for enhanced hydrophilicity and osteoblastic responses. *Mater. Sci. Eng. C Mater. Biol. Appl.* **2017**, *73*, 90–98. [CrossRef] [PubMed]